Theor Chem Acc (2012) 131:1219
DOI 10.1007/s00214-012-1219-6

REGULAR ARTICLE

Tuning of the anion–π interaction

**Antonio Bauzá · David Quiñonero ·
Pere M. Deyà · Antonio Frontera**

Received: 25 January 2012 / Accepted: 4 April 2012 / Published online: 22 April 2012

Abstract In this manuscript, we report an ab initio theoretical study (RI-MP2/aug-cc-pVDZ) that deals with the effect of having different electron acceptor molecules interacting with the aromatic moiety (*s*-triazine) on the anion–π interaction strength. Depending on the type and number of interacting molecules, a wide range of complexation energies can be obtained, and therefore, a tuning of the interaction strength can be adjusted. In addition, cooperativity effects between the anion–π and a variety of other noncovalent and convalent interactions are analyzed and compared. We have used Bader's theory of "atoms-in-molecules" to demonstrate that the electron density computed at the bond critical point that emerges upon complexation can be used not only as a measure of bond order but also as a measure of cooperativity and interplay between the noncovalent interactions that coexist in the same complex.

Keywords Anion–π interactions · Ab initio calculations · Halogen bonding · Lithium bonding · Hydrogen bonding · Cooperativity effects

1 Introduction

In terms of potential applications, supramolecular chemistry has expanded rapidly and integrated backwards into other disciplines, most notably complex nanostructures with astonishing precision. The arrangement and function of supramolecular assemblies take place through a variety of noncovalent forces. An understanding and quantification of intermolecular interactions is of importance both for the rational design of new supramolecular systems, including intelligent materials, as well as for developing new biologically active agents [1]. Noncovalent interactions play a central role in many areas of science and technology, including chemical reactions, molecular recognition and regulation of biochemical processes [2]. These chemical processes are accomplished with specificity and efficiency taking advantage of intricate combinations of weak intermolecular interactions of various sorts. Noncovalent interactions such as hydrogen and halogen bonding, aromatic interactions, and other weak forces govern the organization of multicomponent supramolecular assemblies [3–7]. A deep understanding of these interactions is of great importance for the rationalization of effects observed in several fields, such as biochemistry and materials science. Taking advantage of quantum chemical calculations on model systems, a quantitative and accurate description of these interactions can be achieved [8–10].

There is a variety of noncovalent interactions involving aromatic rings that are very important in supramolecular chemistry [2]. For instance, cation–π [11–16], π–π and CH/π interactions are important factors in molecular recognition and biological processes [3, 17, 18]. In addition, the favorable interaction of anions with π-acidic rings, namely anion–π interaction [19–21], has been extensively studied theoretically [22], and its importance has been corroborated by a great deal of experimental work. For instance, a new family of anion receptors based on anion–π interactions has emerged [23–32]. Moreover, the design and synthesis of highly selective anion channels [33–40]

Electronic supplementary material The online version of this article (doi:10.1007/s00214-012-1219-6) contains supplementary material, which is available to authorized users.

A. Bauzá · D. Quiñonero · P. M. Deyà · A. Frontera (✉)
Departament de Química, Universitat de les Illes Balears,
07122 Palma de Mallorca, Spain
e-mail: toni.frontera@uib.es

represent a very significant progress in this young but consolidated field of the supramolecular chemistry. In addition, the anion–π interaction has been observed in several biological systems. For instance, it participates in the inhibition of the enzyme urate oxidase by cyanide [41] or the enzymatic chlorination of tryptophan by PrnA flavin-dependent halogenase [42]. There are several excellent reviews [43–45] that describe different aspects of the anion–π interaction. From the physicochemical point of view, the anion–π interaction is dominated by electrostatic and anion-induced polarization forces [22]. The strength of the electrostatic component depends upon the value of the quadrupole moment of the arene. The anion-induced polarization term correlates with the molecular polarizability ($\alpha_{\parallel}$) of the aromatic compound [46].

The π-acidity of aromatic rings can be modulated using substituents. The π-electron-rich benzene can be turned into electron poor by substituting hydrogen atoms by electron-withdrawing groups (EWG), for instance nitro groups. This can be named the "covalent way." However, there is another possibility to modulate the π-acidity of the ring, which is the use of noncovalent interactions ("noncovalent way"). This way opens up a wide range of possibilities by using different number and types of interactions that allow a modulation of the π-acidity of the ring. A recent review has examined pairwise combinations of several weak interactions, including anion–π bonding, and described the synergy that operates between them [47]. In particular, the effect of the simultaneous interaction of the aromatic ring with hydrogen and halogen bond donor on the anion–π interaction has been recently studied [48]. In addition, the influence of metal coordination to heteroaromatic rings on the energetics of anion–π interactions has been analyzed in two papers [49, 50]. For instance, the coordination of Ag^{I} has been shown to dramatically enhance their disposition toward anion–π binding [49]. In this manuscript, we report a theoretical study where we analyze the mutual influence of the anion–π interaction with two additional interactions/bonding that have not been studied before, which are interaction with LiF (lithium bonding) and BF_3/BH_3. Lithium, as a congener of hydrogen, undergoes similar interactions to form the lithium bond [51]. Lithium boding is a much less investigated noncovalent interaction than hydrogen bonding. The mutual influence between the lithium and the hydrogen bonds has been recently analyzed [52].

In addition, in this manuscript, we also compare the influence of the aforementioned interactions (lithium bonding, $N\cdots BH_3/BF_3$ interaction) with the already studied influence of the hydrogen, halogen bonding and Ag coordination upon the anion–π interaction. For this study, we have selected *s*-triazine, which is a heteroaromatic ring with three nitrogen atoms that can participate in a variety of interactions as electron donor. Therefore, taking advantage of two factors, that is, the number of nitrogen atoms of the *s*-triazine that participates in σ-bonding and the type of interaction (H, X and Li-bonding, coordination, etc.), a wide range of energies can be obtained and, more importantly, modulated. This can be very important in the design of synthetic receptors for anions or functional material based on this interaction. In addition to the computation of the interaction energies and how they can be adjusted to a desired value, we analyze cooperativity effects by means of two energetic criteria. Moreover, we use the Bader's theory of "atoms-in-molecules," which provides an unambiguous definition of chemical bonding [53], to describe the interactions and to analyze cooperativity effects. The AIM theory has been successfully used to characterize and understand a great variety of interactions including the ones studied herein.

2 Theoretical methods

The geometry[1] of all the complexes included in this study was optimized using the RI-MP2 method and the aug-cc-pVDZ basis set within the program TURBOMOLE version 6.1 [54]. For silver atom, the aug-cc-pVDZPP basis set was used, which uses a relativistic effective core potential (ECP), developed by Peterson and Puzzarini [55]. Specifically, the pseudopotential corresponds to the previously reported Stuttgart/Köln energy consistent PPs that were adjusted to all-electron four-component multi-configuration Dirac–Hartree–Fock calculations, including the two-electron Breit interaction [56]. The RI-MP2 method [57, 58] applied to the study of cation–π and anion–π interactions is considerably faster than the MP2, and the interaction energies and equilibrium distances are almost identical for both methods [59, 60]. We and others have recently demonstrated that this level of theory gives comparable results to the CCSD(T)/AVTZ//RI-MP2/aug-cc-pVQZ level for several anion–π complexes [61, 62]. The binding energy (E) was calculated at the same level with correction for the basis set superposition error (BSSE) using the counterpoise method [63]. The optimization of the molecular geometries has been performed imposing the C_{3v} symmetry point group, unless otherwise noted. Other possible conformations of complexes have not been considered because the ultimate aim of this study is to analyze the π-binding properties of coordinated *s*-triazine toward anions. If the optimization is carried out without imposing

---

[1] Cartesian coordinates of the RI-MP2/aug-cc-pVDZ optimized structures of all compounds and complexes are available for download from the Theoretical Chemistry Accounts supplementary material website: http://www.springer.com.

symmetry constrains, a migration of the anion to the interacting molecules is observed. The final result is the anion "solvated" by the σ-interacting molecules. For several complexes, where the BSSE correction was very large, we have carried out BSSE-corrected geometry optimizations in order to know the influence of the BSSE on the geometry of the complex. The "atoms-in-molecules" analysis [64] has been performed by means of the AIM2000 version 2.0 program [65] using the MP2/aug-cc-pVDZ wave functions. We have used the Merz–Kollman scheme for deriving atomic charges and studying charge transfer effects at the same level of theory. It has been reported that this method provides high-quality charges [66].

In the multicomponent complexes where anion–π and other interactions coexist, we have studied cooperativity effects by computing the cooperativity energy E_{coop} using Eq. (1).

$$E_{\text{coop}} = E_{\text{BSSE}}(\text{A}\pi + \sigma\text{B}) - E_{\text{BSSE}}(\text{A}\pi) - E_{\text{BSSE}}(\sigma\text{B}) - E_{\text{BSSE}}(\text{AB}) \qquad (1)$$

where $E_{\text{BSSE}}(\text{A}\pi)$, $E_{\text{BSSE}}(\sigma\text{B})$ and $E_{\text{BSSE}}(\text{A}\pi + \sigma\text{B})$ terms correspond to the interaction energies (BSSE-corrected) of the corresponding optimized anion–π, σB (this notation is used to define any interaction involving the nitrogen atoms of the ring, which are almost coplanar with the ring) and multicomponent anion–π + σB complexes, respectively. The $E_{\text{BSSE}}(\text{AB})$ term is the interaction of the anion with the molecules that interact with the nitrogen atoms in the geometry that they have in the anion–π–σB complexes (in the absence of the π-system). This expression has been successfully used in the study of cooperativity effects in a variety of systems in which two different interactions coexist, including π systems as simultaneous hydride- and hydrogen-bond acceptors and the simultaneous interaction of tetrafluoroethene with anions and hydrogen-bond donors [47].

3 Results and discussion

3.1 Preliminary findings and results

We have examined the Cambridge Structural Database in order to find evidences of anion–π interactions in systems where the aromatic ring is establishing simultaneous interactions either with boron or alkaline atoms. While experimental evidences of simultaneous interaction of electron-deficient aromatic compounds with anions and hydrogen and halogen bond donors, and coordination to Ag^{I} have been reported [22], the possibility of interaction with anions and boron or alkaline derivatives has not been studied so far. There is a significant number (>40) of X-ray structures containing electron-deficient heteroaromatic rings interacting with anions where the nitrogen atom is bonded to boron at the same time. In contrast, the number is significantly reduced (<5) when the boron is replaced by any alkaline atom. Three selected examples are shown in Fig. 1. For the anion–π complexes where the aromatic ring is coordinated to boron, we show two structures, GUKSEK [67] and BOQSOP [68], where interesting anion–π interactions are present. Finally, in the VEPBUO [69] structure, the heteroaromatic 1,10-phenanthroline rings are interacting with a sodium cation in a 3:1 stoichiometry. Adduct is establishing two anion–π interactions with the trifluoromethanesulfonate anion.

In addition to the CSD search, we have also performed some preliminary calculations computing the molecular electrostatic potential (MEP) surface of *s*-triazine alone and coordinated to the molecules used to increment the π-acidity of the ring by means of their interaction with the aromatic nitrogen atoms (see Fig. 2). From the MEP results, it is clear that the influence of the interacting molecules on the π-acidity of the ring is strong. Furthermore, the wide range of MEP energies obtained for the *s*-triazine complexes anticipates a possible modulation of the interaction playing with both the type and number of σ-interactions.

3.2 Anion–π and σ complexes

Table 1 summarizes the interaction energies without and with BSSE correction (E and E_{BSSE}, respectively) and equilibrium distances of complexes **2–10** (see Fig. 3) at the MP2/aug-cc-pVDZ level of theory. The interaction energies of anion–π complexes **2–4** follow the general trend regarding energies and distances expected for halide anions. As a matter of fact, the *s*-triazine ring has an almost negligible quadrupole moment ($Q_{zz} = 0.90$ B), and consequently, the interaction with anions or lone pairs of electronegative atoms is not electrostatically very favored, and the interaction is dominated by polarization effects. Concerning the σ-interactions, we can divide them into covalent and noncovalent. The model molecules used to study these interactions are neutral. For the noncovalent hydrogen, halogen and lithium bonds, we have used HF, BrF and LiF molecules, respectively. To model the interaction with transition metal complexes, we have used AgCl. Finally, for the interaction with boron, we have used BH_3 and BF_3 molecules. Curiously, the halogen bonds (complex **6**) are stronger than the hydrogen bonds (**5**) and even higher than the lithium bonds (**7**). For the covalent bonds, the Ag–N bond is stronger than the B–N bond.

Fig. 1 Partial view of the X-ray structures retrieved from the CSD. The hydrogen atoms have been omitted for the sake of clarity. Distances in Å

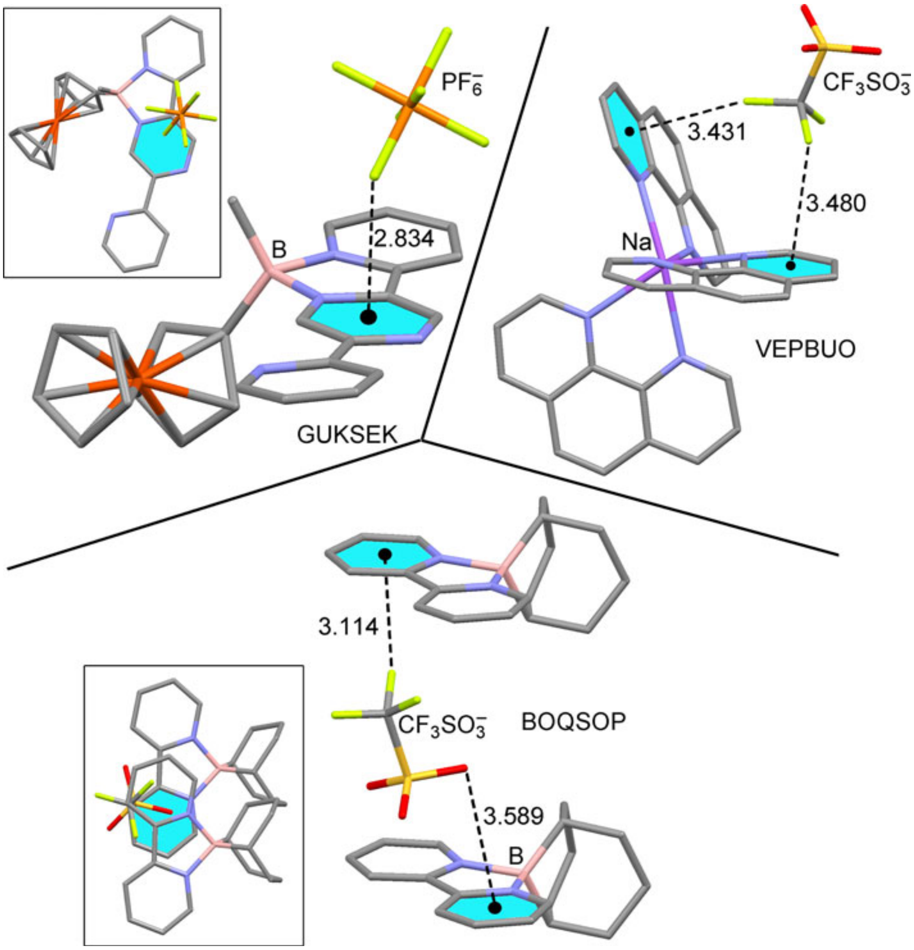

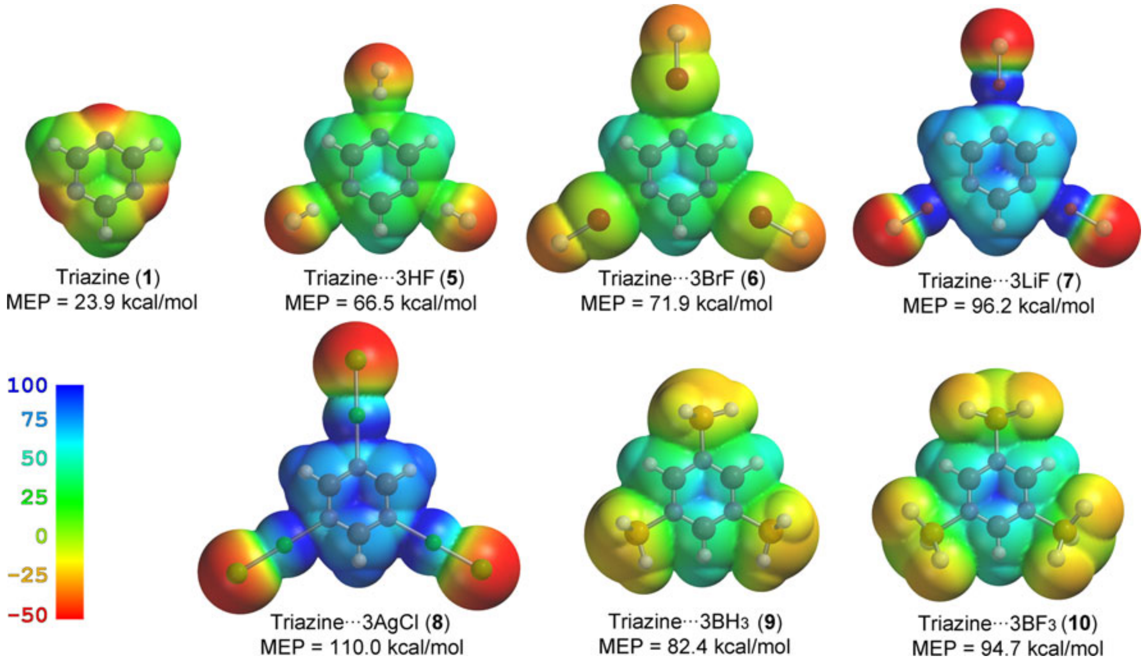

Fig. 2 MEP surfaces of triazine alone and σ-bonded (coordinated) to several molecules. Legend energies in kcal/mol

Table 1 Interaction energies with BSSE correction (E_{BSSE} in kcal/mol) and equilibrium distances (R, Å) at RI-MP2/aug-cc-pVDZ level of theory for complexes **2**–**10**

Complex	E_{BSSE}	R	Q_{MK}	$10^2\rho$
2 (**1** + F^-)	−10.6	2.542	−0.84	0.9998
3 (**1** + Cl^-)	−7.0	3.145	−0.89	0.6974
4 (**1** + Br^-)	−6.1	3.333	−0.91	0.6325
5 (**1** + 3HF)	−22.4	1.774		3.9644
6 (**1** + 3BrF)	−30.2	2.385		4.8210
7 (**1** + 3LiF)	−27.8	2.102		2.2229
8 (**1** + 3AgCl)	−68.5	2.098		9.1372
9 (**1** + $3BH_3$)	−65.8	1.665		9.0496
10 (**1** + $3BF_3$)	−27.0	1.777		8.1628

Merz–Kollman-derived charges (Q_{MK}, e) of the anion (complexes **2**–**4**) and the values of the charge density at the bond (complexes **5**–**10**) or cage CP (complexes **2**–**4**) (ρ, a.u.) are also summarized

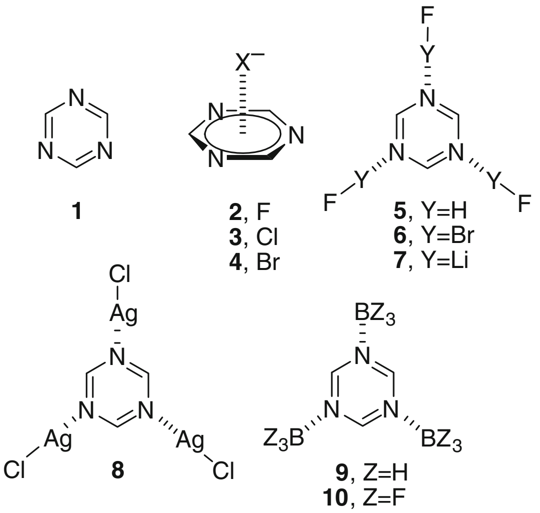

Fig. 3 Compound **1** and their complexes **2**–**10**

3.3 Cooperativity in multicomponent anion–π and σ-bonded complexes

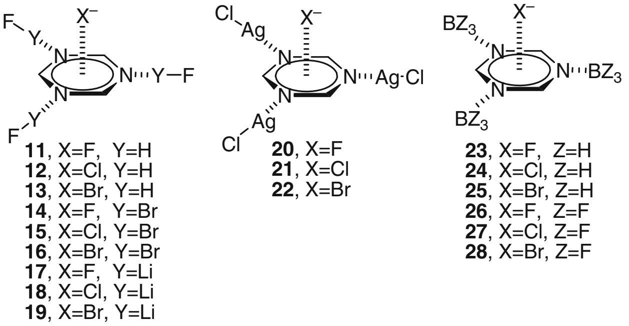

Fig. 4 Multicomponent anion–π and σ-bonded complexes **11**–**28**

The geometric and energetic results computed for multicomponent complexes **11**–**28** (see Fig. 4) are summarized in Table 2. For two complexes, where the BSSE energies are large (**18** and **19**), we have carried out BSSE-corrected geometry optimizations, and we have obtained comparable results, very similar interaction energies and slightly larger equilibrium distances. For complexes where the nitrogen atoms of *s*-triazine are forming covalent bonds with silver and boron (**20**–**28**), the BSSE correction has not been applied. Some interesting points can be extracted from the geometrical results. The equilibrium distance R_e of the anion–π interaction in anion–π–σB complexes is shorter than in binary complexes **2**–**4;** that is, the presence of any of the other interactions (sigma bonds) studied in this work strengthens the anion–π interaction. In addition, the equilibrium distances of the σ-bonding interaction $R_{\sigma B}$ is also shorter in anion–π–σB complexes compared to complexes **5**–**10;** that is, the presence of the anion–π interaction also strengthens the σ-bonding interaction. As expected, this mutual reinforcement varies depending on the kind of σ-interaction. In general, the shortening of the anion–π interaction ($0.189 \leq \Delta R_e \leq 0.396$ Å) is more significant than the shortening of the σ-interaction ($0.007 \leq \Delta R_{\sigma B} \leq 0.156$ Å), which likely indicates that the anion–π interaction is more reinforced than the σ-interaction. This issue will be further discussed below. The greater shortening of the $R_{\sigma B}$ values corresponds to the hydrogen, halogen bonding and N···BF_3 interactions.

It should be emphasized that the values of E_{BSSE}(AB) energies summarized in Table 2 are very large, indicating that the interaction of the anion with the σ-bonded molecules is very important in the multi-component complexes, particularly in fluoride complexes where the distance from the anion to the σ-bonded molecules is shorter. Therefore, this interaction has a strong influence in the formation of the complexes. This is the reason why it is very important to subtract this value from the total interaction energy when computing the cooperativity energies.

At this point, it is interesting to analyze our results taking into account the recent work published by Wheeler and Houk [70], regarding the nature of anion–π interactions involving benzene rings. Although it is difficult to apply in heteroaromatic rings [71], it represents an interesting and different way to explain the effect of the substituents on the anion–π strength. They propose that substituent effects in these systems can be attributed mainly to direct interactions between the anion and local C–X dipoles. Specifically, interaction energies for $Cl^-\cdots C_6H_{6-n}X_n$ complexes could be matched using a model system in which the substituents are isolated from the aromatic ring and π–resonance effects are impossible. Wheeler and Houk demonstrate that the interaction energy for $Cl^-\cdots C_6H_{6-n}X_n$ complexes follows a linear relationship with the electrostatic potential

Table 2 Interaction energies and cooperativity energies with BSSE correction (E_{BSSE} and E_{coop}, respectively, in kcal/mol), equilibrium distances (R_e and $R_{\sigma B}$, in Å) and their variation (ΔR_e and $\Delta R_{\sigma B}$, in Å) at the RI-MP2/aug-cc-pVDZ level of theory for complexes **11**–**28**

Complex	E^a_{BSSE}	E_{coop}	E_{BSSE} (AB)	R_e	$R_{\sigma B}$	ΔR_e	$\Delta R_{\sigma B}$
11	−57.0	−7.3	−16.7	2.353	1.656	0.189	0.118
12	−48.2	−5.6	−13.2	2.929	1.685	0.216	0.089
13	−45.9	−5.1	−12.3	3.110	1.693	0.223	0.081
14	−76.8	−20.8	−15.2	2.255	2.229	0.287	0.156
15	−65.2	−16.0	−12.0	2.817	2.252	0.328	0.133
16	−62.2	−14.6	−11.3	2.993	2.258	0.340	0.127
17	−90.9	−5.8	−46.7	2.271	2.043	0.271	0.059
18	−78.4	−5.6	−38.0	2.822	2.059	0.323	0.043
	−79.0			*2.878*	*2.129*		
19	−75.0	−5.4	−35.7	2.995	2.063	0.338	0.039
	−75.7			*3.059*	*2.134*		
20	−136.0	−10.0	−46.9	2.227	2.086	0.315	0.012
21	−122.6	−7.1	−40.0	2.779	2.090	0.366	0.008
22	−119.0	−6.0	−38.4	2.951	2.091	0.382	0.007
23	−109.5	−15.7	−17.4	2.260	1.642	0.282	0.023
24	−97.7	−12.1	−12.8	2.824	1.646	0.321	0.019
25	−94.7	−11.2	−11.6	3.000	1.647	0.333	0.018
26	−82.0	−15.2	−29.2	2.190	1.672	0.352	0.105
27	−67.0	−12.1	−20.9	2.761	1.689	0.384	0.088
28	−63.2	−11.2	−18.9	2.937	1.694	0.396	0.083

The E_{BSSE}(AB) values as defined in Eq. (1) in kcal/mol are also summarized. R_e is the anion–π equilibrium distance, and $R_{\sigma B}$, the equilibrium distance of the σ-bonding interaction

[a] Values in italics correspond to BSSE-corrected geometry optimization results

evaluated at the position of Cl^-. The resulting equation has a scaling factor between the interaction energy and E_{ele} close to 1 ($E = 0.98*E_{ele} - 7.27$). Therefore, the differences in the interaction energy of the complexes reflect the differences in the electrostatic contribution to the total interaction energy. This explanation has been also used by Wheeler and Houk in other systems and interactions like cation–π and π–π stacking [72, 73]. We have recently applied this analysis to anion–π complexes of fluorinated ethyne, ethene, butadiene, benzene and [n]radialenes ($n = 3$–5) [74] where we have successfully used the Wheeler–Houk correlation. We have shown that the differences in interaction energy mainly reflect the differences in the electrostatic term. In this work, inspired by the manuscript of Wheeler and Houk [70], we have represented the total interaction energy obtained for noncovalent complexes **11**–**19** versus the E_{BSSE}(AB) term, which accounts for the interaction of the halogen anion with the three sigma-complexing agents in their complex geometry in the absence of *s*-triazine. We have found a very modest relationship ($R^2 = 0.63$, see Fig. 5), which likely means that the changes in the interaction energies of the multicomponent complexes reflect to some extent the differences between the interactions of the anion with the σ-interacting molecules. In this case, the resulting equation obtained from the regression plot has a scaling factor of 0.86, confirming that the energetic trend observed in complexes **11**–**19** only in part reflects the differences in E_{BSSE}(AB) values. Moreover, if all complexes are included in the representation, a complete scatter of point is observed ($R^2 = 0.001$, see Fig. 5). Therefore, other factors can be important apart from the interaction of the anion with the σ-molecules in the covalent complexes. For instance, in the complexes involving BH_3 and BF_3 molecules, there is a change of hybridization of the boron atom upon complexation, and consequently, the geometry of the "σ-molecule" changes significantly. Therefore, the interaction energies of the multicomponent complexes involving these molecules are affected by other influences that are not present in the noncovalent complexes **11**–**19**.

Table 2 also lists the computed values of cooperativity energies E_{coop} [see Eq. (1)], which are intended to provide an estimation of the "extra" energetic stabilization or destabilization obtained in multicomponent complexes as a consequence of the coexistence of both interactions. From the E_{coop} values listed in Table 2, several general conclusions can be extracted. First, the values of E_{coop} are negative in all complexes, thus indicating a positive synergy between the interactions, in agreement with shortening of the equilibrium distances (see ΔR values of Table 2). Second, in absolute terms, the E_{coop} values are important in all complexes **11**–**28** (anion–π–σB assemblies) contributing 5–30 % of the total interaction energy. Unexpectedly, the E_{coop} values are more significant in halogen bonding than hydrogen-bonding complexes. This points out that the

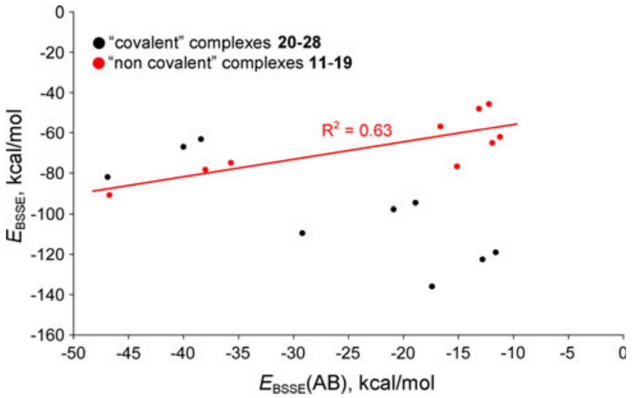

Fig. 5 Regression plot of the total interaction energy (E_{BSSE}) versus the interaction of the anion with the interacting σ-molecules in their complex geometry in the absence of *s*-triazine (E_{BSSE}(AB), see Eq. 1) for complexes **11**–**28**

interaction of the halogen-bonding donor molecules with the lone pair of the nitrogen atoms by means of the σ-hole of the bromine atom increases the π acidity of the *s*-triazine to a major extent. The computed values of E_{coop} for complexes **23–28** are also remarkable, in which the presence of strong Lewis acid groups has a strong influence on the anion–π interaction. It also is interesting to note that the capability of BH_3 molecule to increase the π-acidity of the *s*-triazine is greater than that of BF_3. As a matter of fact, the binding energy of *s*-triazine and three molecules of BH_3 is almost 30 kcal/mol more favorable than the interaction with three molecules of BF_3 (see Table 1). This result is in agreement with previous theoretical [75] and experimental results [76], which have shown that BF_3 is a weaker Lewis acid than BH_3. In fact, the experimental B–N bond strengths of $Me_3N–BH_3$ and $Me_3N–BF_3$ compounds are 38.3 and 31.0 kcal/mol, respectively [76].

To investigate whether cooperativity effects can be related to charge transfer from the anion to the aromatic system, the Merz–Kollman charges on the anion in the complexes are summarized in Table 3. This method for deriving atomic charges is expected to give good quality charges [66]. To study the relationship between charge transfer and cooperativity effects, the variation of the anion charge in multicomponent systems **11–28** with respect to the binary anion–π complexes **2–4** is summarized in Table 3 (ΔQ_{MK} values). In all complexes, ΔQ_{MK} is positive, that is, anion → π charge transfer is greater in anion–π–σB complexes than in anion–π complexes **2–4**. Therefore, this can be understood as an indication of reinforcement of the anion–π interaction, in agreement with the E_{coop}, ΔR_{e} and $\Delta R_{\sigma \mathrm{B}}$ values. We have also analyzed whether there is a correlation between the cooperativity values (E_{coop}) and the total interaction energy (E) in complexes **11–28;** however, a dispersion of points lacking any correlation has been found (see Figure S1 in the supplementary material), indicating that the cooperativity energy is not related to the total interaction energy of the multicomponent complexes.

Table 3 Anion charges (Q, e) and their variation (ΔQ, e), according to the Merz–Kollman (MK) method

Compound	Q_{MK}	ΔQ_{MK}	ρ_{CCP}	ρ_{BCP}	$\Delta\rho_{\mathrm{CCP}}$	$\Delta\rho_{\mathrm{BCP}}$
11	−0.80	0.04	1.3082	5.4849	3.085	15.205
12	−0.86	0.04	0.9619	5.0571	2.646	10.928
13	−0.87	0.04	0.8846	4.9518	2.520	9.874
14	−0.76	0.08	1.5031	6.9384	5.033	21.174
15	−0.80	0.10	1.1436	6.5714	4.462	17.504
16	−0.81	0.09	1.0626	6.4768	4.3	16.558
17	−0.77	0.07	1.4659	2.6428	4.662	4.199
18	−0.80	0.09	1.1271	2.5267	4.297	3.037
19	−0.81	0.10	1.0504	2.4987	4.179	2.758
20	−0.73	0.11	1.5465	9.5443	5.468	4.072
21	−0.77	0.13	1.1995	9.4174	5.021	2.803
22	−0.77	0.14	1.1223	9.3887	4.898	2.516
23	−0.83	0.00	1.4745	9.9313	4.748	8.818
24	−0.86	0.04	1.1232	9.7329	4.258	6.833
25	−0.86	0.05	1.0451	9.6939	4.126	6.433
26	−0.81	0.03	1.6148	10.5235	6.151	23.607
27	−0.82	0.07	1.2272	10.0467	5.298	18.839
28	−0.82	0.09	1.1417	9.9387	5.092	17.759

The values of the charge density ($10^2\rho$) at cage and bond CPs (CCP and BCC, respectively) and its variation ($\Delta\rho$) at the MP2/aug-cc-pVDZ level of theory for complexes **11–28** are given in a.u

3.4 AIM analysis

We performed the AIM analysis of all compounds studied in this work. It is well established that the charge density ρ at the critical points (CPs) that emerge upon complexation give helpful information regarding the strength of the noncovalent interactions involved in the complexes [46, 77]. Indeed they have been successfully used as a measure of the bond order in a variety of noncovalent interactions including anion–π and hydrogen-bonding and halogen-bonding interactions [48, 78, 79]. Therefore, the variation in the ρ value at CPs in multicomponent systems with respect to the isolated anion–π and σB complexes can be used to analyze the mutual influence of the two interactions. One example that involves a classical noncovalent interaction and other that involves a coordination dative bond are illustrated in Fig. 6. Anion–π–HB complex **11** has a ρ value of 5.4849×10^{-2} a.u. at the bond CP that characterizes the hydrogen-bonding interaction, which is greater than the value computed at the bond CP of complex **5** (3.9644×10^{-2} a.u.). This result confirms that the hydrogen bond in **11** is reinforced with respect to complex **5**. The same behavior is observed for the values of ρ at the cage CP that characterizes the anion–π interaction. Variation of this value from 0.9998×10^{-2} a.u. for complex **2** to 1.3082×10^{-2} a.u. for complex **11** indicates reinforcement of the anion–π interaction. Similarly, both interactions are also strengthened in complex **24** ($\sigma B = BH_3$) with respect to complexes **3** and **9**. For the rest of the complexes, similar conclusions can be extracted (see Table 3). In all anion–π–σB complexes, the $\Delta\rho$ values are positive, thus indicating reinforcement of both interactions, in agreement with the energetic, charge transfer and geometric results. The variation of the ρ values at the cage and bond CPs ($\Delta\rho_{\mathrm{e}}$ and $\Delta\rho_{\sigma \mathrm{B}}$ values) can be used as a degree of strengthening of the interaction. For instance, the variation of the ρ value at the cage CP in complex **24** is greater than in complex **11** indicating that the anion–π interaction is more reinforced in **24** than in **11**, as expected considering the strong Lewis acid character of the BH_3 molecule.

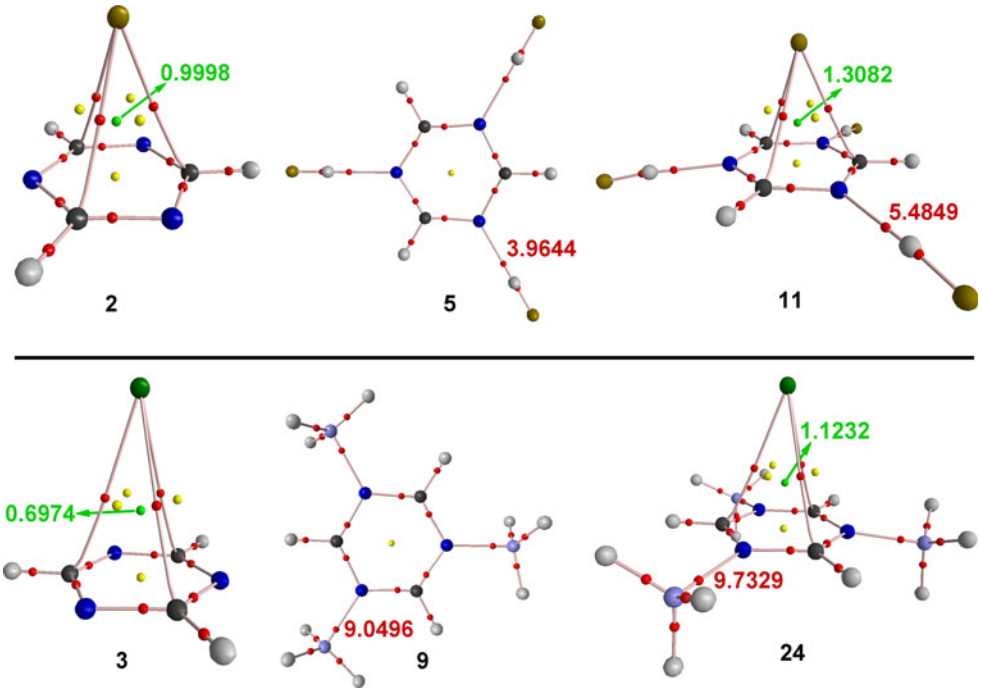

Fig. 6 Distribution of critical points in some anion–π, σB and anion–π–σB complexes (bond CPs in *red*, ring CPs in yellow and cage CPs in *green*). The values of $10^2\rho$ for bond and cage CPs are shown in *red* and *green*, respectively. Values in a.u

3.5 Mutual influence between anion–π and σB noncovalent interactions

In an attempt to evaluate not only the effect of the any σ-bonding on the anion–π interaction and vice versa but also which of the two interactions is more reinforced, we computed the binding energy of the multicomponent complexes using two different approaches (see Fig. 7). First, we computed the interaction energies of the X^-–π–σB complexes (see Table 4), considering that the σ-bonded complex has been previously formed and evaluating the interaction with the anion as a two-component system (e.g., **5** + $F^- \rightarrow$**11**), denoted $E_{A\pi\_2}$. Second, we computed the interaction energies of multicomponent complexes X^-–π–σB, considering that the anion–π complex has been previously formed and evaluating its interaction with the σ-bonding donor molecules (e.g., **2** + 3HF → **11**), denoted $E_{\sigma B\_2}$. Finally, we compared the quantities $E_{\sigma B\_2}$ and $E_{A\pi\_2}$ with the $E_{\sigma B\_1}$ and $E_{A\pi\_1}$ binding energies, which correspond to the binding energies of complexes **2–10** (see Table 1), by using the ratios $E_{\sigma B\_2}/E_{\sigma B\_1}$ and $E_{A\pi\_2}/E_{A\pi\_1}$. These simple ratios give very interesting and useful information: (1) values of $E_{\sigma B\_2}/E_{\sigma B\_1} > 1$ mean that the σ-bonding is reinforced in the anion–π–σB complex and vice versa for $E_{\sigma B\_2}/E_{\sigma B\_1} < 1$; (2) values of $E_{A\pi\_2}/E_{A\pi\_1} > 1$ mean that the anion–π interaction is reinforced in the anion–π–XB complex and vice versa if $E_{A\pi\_2}/E_{A\pi\_1} < 1$. Therefore, these ratios are informative regarding the mutual influence of the two interactions in the anion–π–σB complexes. If both ratios are greater than unity, favorable synergetic effects between the two interactions are present in the complex. If one ratio is greater than unity and the other lesser than unity, this would mean that one noncovalent interaction is reinforced at the expense of the other. More significantly, for a given complex, $E_{\sigma B\_2}/E_{\sigma B\_1} > E_{A\pi\_2}/E_{A\pi\_1}$ would mean that the

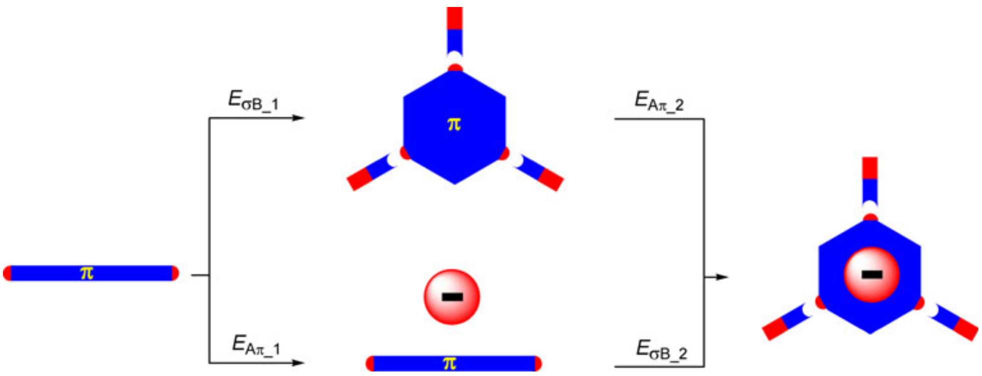

Fig. 7 Schematic representation of the two routes to form the anion–π–σB complexes that allow computation of the $E_{A\pi\_2}/E_{A\pi\_1}$ and $E_{\sigma B\_2}/E_{\sigma B\_1}$ ratios

Table 4 $E_{A\pi\_2}$, E_{XB_2}, $E_{A\pi\_2}/E_{A\pi\_1}$ and $E_{\sigma B\_2}/E_{\sigma B\_1}$ values computed for several complexes at the MP2/aug-cc-pVDZ level of theory

Complex	Reaction	$E_{A\pi\_2}$	$E_{A\pi\_2}/E_{A\pi\_1}$	Reaction	$E_{\sigma B\_2}$	$E_{\sigma B\_2}/E_{\sigma B\_1}$
11	**5** + F^-	−37.7	3.0	**2** + 3HF	−52.1	2.0
12	**5** + Cl^-	−28.7	3.4	**3** + 3HF	−46.9	1.8
13	**5** + Br^-	−26.6	3.4	**4** + 3HF	−45.5	1.7
14	**6** + F^-	−51.4	4.2	**2** + 3BrF	−77.3	2.0
15	**6** + Cl^-	−39.4	4.7	**3** + 3BrF	−69.2	1.8
16	**6** + Br^-	−36.7	4.7	**4** + 3BrF	−67.1	1.8
17	**7** + F^-	−67.1	5.5	**2** + 3LiF	−99.6	2.2
18	**7** + Cl^-	−54.5	6.5	**3** + 3LiF	−90.9	2.0
19	**7** + Br^-	−51.4	6.6	**4** + 3LiF	−88.5	2.0
20	**8** + F^-	−70.5	5.7	**2** + 3AgCl	−141.4	1.7
21	**8** + Cl^-	−57.1	6.8	**3** + 3AgCl	−132.0	1.6
22	**8** + Br^-	−54.1	7.0	**4** + 3AgCl	−129.5	1.6
23	**9** + F^-	−46.3	3.8	**2** + $3BH_3$	−110.1	1.5
24	**9** + Cl^-	−34.6	4.1	**3** + $3BH_3$	−102.3	1.3
25	**9** + Br^-	−32.1	4.1	**4** + $3BH_3$	−100.4	1.3
26	**10** + F^-	−59.3	4.8	**2** + $3BF_3$	−94.1	2.0
27	**10** + Cl^-	−44.2	5.3	**3** + $3BF_3$	−83.0	1.8
28	**10** + Br^-	−41.0	5.3	**4** + $3BF_3$	−80.3	1.7

The $E_{A\pi\_1}$ and E_{XB_1} values are taken from Table 1. Energies are given in kcal/mol

halogen-bonding interaction is more reinforced than the anion–π interaction in the anion–π–σB complex, and the contrary applies if $E_{\sigma B\_2}/E_{\sigma B\_1} < E_{A\pi\_2}/E_{A\pi\_1}$. If the two ratios are equal, the reinforcement of both interactions is the same. These relationships have been previously used by us and others [78, 80] to study cooperativity effects.

The values of $E_{A\pi\_2}$, E_{XB_2}, $E_{A\pi\_2}/E_{A\pi\_1}$ and $E_{\sigma B\_2}/E_{\sigma B\_1}$ computed for multicomponent complexes **11–28** are summarized in Table 4. Both ratios are greater than unity in all complexes, in agreement with the previously discussed energetic and geometric results. In addition, for all complexes, $E_{A\pi\_2}/E_{A\pi\_1}$ is much greater than $E_{\sigma B\_2}/E_{\sigma B\_1}$; that is, the anion–π interaction is more enhanced than any of the σ-bonding interactions, in agreement with the ΔR_e and $\Delta R_{\sigma B}$ values. These interesting results allow us to learn which interaction in the multicomponent system is more reinforced. This information cannot be obtained from the cooperativity energies E_{coop} or AIM analysis.

3.6 Tuning of the interaction in multicomponent complexes

Taking advantage of the modulation of the anion–π strength achieved using either the hydrogen/halogen/lithium bond acceptor ability of the nitrogen atoms of the *s*-triazine or the coordination to metal or Lewis acid molecules, a tuning of the interaction can be envisaged. We have extended our study computing the interaction energies of the *s*-triazine mono- and di-coordinated to the σ-bonding molecules (HF, BrF, AgCl, LiF, BH_3 and BF_3) in order to use the additional versatility provided by number of N atoms of the heteroaromatic ring. We have gathered in Table 5 the $E_{rA\pi\_2}$ values for all *s*-triazine compounds (mono-, di- and tri-coordinated) interacting with F^-, Cl^- and Br^- ions, relative to complexes **2-4**. It can be observed that the relative interaction energies range from −7.7 to −58.2 kcal/mol for F^-, from −6.1 to −48.7 for Cl^- and from −5.7 to −46.3 kcal/mol for Br^-. Interestingly, the interaction strength can be adjusted for the three anions. For instance, depending on the σ-interaction and the number of nitrogen atoms that participates, we have six possibilities to adjust the interaction between 10 and 20 kcal/mol for the F^- complexes. Similarly, we have five possible combinations to adjust the interaction energy between 20 and 30 kcal/mol for Cl^- and Br^- anions. In Fig. 8, we have represented the relative interaction energies computed for each series of anions. It can be appreciated that the interaction can be modulated using both the type of the σ-interaction and the number of nitrogen atoms participating in it. Cl^- and Br^- present similar interaction energies, and F^- presents more favorable binding energies. Moreover, the difference between F^- and the other two anions is not constant, and it increases as the interaction energy becomes more negative.

It should be mentioned that the results reported herein are obtained using gas-phase calculations. It is difficult to extrapolate the results in order to interpret the properties of solid-state systems. It is clear that the mutual influence between the different noncovalent interactions in the solid state is much lower than in gas phase. Hopefully, this study will contribute to understand the different and delicate combination of noncovalent forces that governs, in most cases, the fascinating and unpredictable architecture of solids. It should be also mentioned that the focus of the study is to elucidate trends, not predict exact results. The results are thus valid for the gas phase and the trends likely hold true, though interaction energies would be much lower, in the solid phase. However, the values or trends are probably not applicable to aqueous or highly polar solution phases.

4 Concluding remarks

The results reported in this manuscript stress the importance of the mutual effects between noncovalent interactions involving aromatic systems, namely anion–π and hydrogen, halogen and lithium bonding, which can lead to strong cooperativity effects. These effects are even more important in systems where the nitrogen atom is directly coordinated to metal ions or to BH_3. We estimated the

Table 5 Relative binding energies ($E_{rA\pi\_2}$, in kcal/mol) (R_e, in Å) at the RI-MP2/aug-cc-pVDZ level of theory for mono-, di- and tri-coordinated *s*-triazine

Compound	F^-			Cl^-			Br^-		
	$E_{rA\pi\_2}$	R_e	ρ (3, +3)	$E_{rA\pi\_2}$	R_e	ρ (3, +3)	$E_{rA\pi\_2}$	R_e	ρ (3, +3)
TAZ	0.0	2.542	0.9998	0.0	3.145	0.6974	0.0	3.333	0.6325
TAZ·HF	−7.7	2.479	1.0791	−6.1	3.073	0.7753	−5.7	3.259	0.7035
TAZ·2HF	−15.6	2.416	1.1740	−12.3	3.001	0.8602	−11.5	3.184	0.7923
TAZ·3HF	−25.4	2.353	1.3083	−20.2	2.929	0.9620	−18.9	3.110	0.8846
TAZ·BrF	−13.9	2.446	1.1313	−11.0	3.036	0.8174	−10.2	3.220	0.7530
TAZ·2BrF	−25.1	2.351	1.2996	−20.0	2.926	0.9607	−18.7	3.106	0.8886
TAZ·3BrF	−39.1	2.255	1.5031	−31.0	2.817	1.1436	−29.0	2.993	1.0626
TAZ·LiF	−17.4	2.452	1.1272	−14.5	3.037	0.8136	−13.6	3.220	0.7493
TAZ·2LiF	−35.3	2.361	1.2764	−29.6	2.930	0.9558	−28.0	3.108	0.8822
TAZ·3LiF	−54.8	2.271	1.4659	−46.0	2.822	1.1271	−43.6	2.995	1.0505
TAZ·AgCl	−19.9	2.437	1.1447	−16.3	3.023	0.8407	−15.3	3.206	0.7648
TAZ·2AgCl	−39.0	2.332	1.3289	−32.3	2.901	1.0024	−30.6	3.078	0.9271
TAZ·3AgCl	−58.2	2.227	1.5465	−48.7	2.779	1.1996	−46.3	2.951	1.1224
TAZ·BH_3	−11.0	2.448	1.1283	−8.4	3.038	0.8158	−7.7	3.222	0.7517
TAZ·2BH_3	−21.8	2.354	1.2929	−16.7	2.931	0.9593	−15.4	3.111	0.8959
TAZ·3BH_3	−34.0	2.260	1.4745	−26.2	2.824	1.1232	−24.3	3.000	1.0451
TAZ·BF_3	−14.8	2.425	1.1773	−11.0	3.017	0.8426	−10.0	3.201	0.7771
TAZ·2BF_3	−28.7	2.307	1.3182	−20.0	2.889	0.9721	−19.6	3.069	0.8979
TAZ·3BF_3	−47.0	2.190	1.6148	−31.0	2.761	1.2272	−33.1	2.937	1.1418

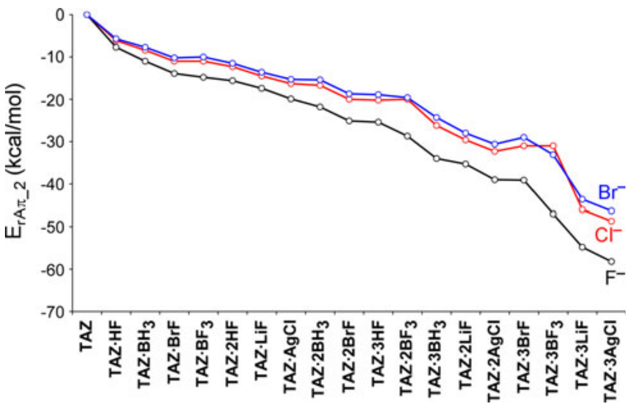

Fig. 8 Representation of the relative interaction energies of F^- (*black line*), Cl^- (*red line*) and Br^- (*blue line*) complexes

cooperativity effects energetically (E_{coop} values), obtaining results that are in agreement with the geometric features of the complexes and the AIM analysis.

The modest correlation obtained between the cooperativity energy (E_{coop}) and the interaction energy between the halogen anion and the N-substituent in the absence of *s*-triazine, (E_{BSSE}(AB)) indicates that the cooperativity effect is to some extent due to an enhancement of the anion–π and σ interactions, but also due to a direct interaction between the halogen anion and the N-substituent.

Finally, taking advantage of the type of σ-interaction and number of nitrogen atoms that participate in the σ-bond, we are able to adjust the interaction to a given value. This can be useful to design anion receptors or other anion-sensing devices based on this interaction.

Acknowledgments We thank CONSOLIDER–Ingenio 2010 (CSD2010-0065) and the MICINN of Spain (project CTQ2011-27512/BQU, FEDER funds) for financial support. D.Q. thanks the MICINN of Spain for a "Ramon y Cajal" contract. We thank the CESCA for computational facilities.

References

1. Schneider H-J (2009) Angew Chem Int Ed 48:3924
2. Meyer EA, Castellano RK, Diederich F (2003) Angew Chem Int Ed 42:1210
3. Dougherty DA (1996) Science 271:163
4. Kim KS, Tarakeshwar P, Lee (2000) J Y. Chem Rev 100:4145
5. Lee EC, Kim D, Jureèka P, Tarakeshwar P, Hobza P, Kim KS (2007) J Phys Chem A 111:3446
6. Reddy AS, Sastry GN (2005) J Phys Chem A 109:8893
7. Cerný J, Hobza P (2007) Phys Chem Chem Phys 9:5291
8. Rappé AK, Bernstein ER (2000) J Phys Chem A 104:6117
9. Hesselmann A, Jansen G, Schütz M (2006) J Am Chem Soc 128:11730
10. Piacenza M, Grimme S (2005) Chem Phys Chem 6:1554
11. Ma JC, Dougherty DA (1997) Chem Rev 97:1303

12. Gallivan JP, Dougherty DA (1999) Proc Natl Acad Sci USA 96:9459
13. Gokel GW, Wall SLD, Meadows ES (2000) Eur J Org Chem 2967
14. Gokel GW, Barbour LJ, Wall SLD, Meadows ES (2001) Coord Chem Rev 222:127
15. Gokel GW, Barbour LJ, Ferdani R, Hu J (2002) Acc Chem Res 35:878
16. Hunter CA, Singh J, Thorton JM (1991) J Mol Biol 218:837
17. Kumpf RA, Dougherty DA (1993) Science 261:1708
18. Heginbotham L, Lu Z, Abramson T, Mackinnon R (1994) Biophys J 66:1061
19. Mascal M, Armstrong A, Bartberger M (2002) J Am Chem Soc 124:6274
20. Alkorta I, Rozas I, Elguero J (2002) J Am Chem Soc 124:8593
21. Quiñonero D, Garau C, Rotger C, Frontera A, Ballester P, Costa A, Deyà PM (2002) Angew Chem Int Ed 41:3389
22. Frontera A, Quiñonero D, Deyà PM (2011) WIREs Comput Mol Sci 1:440
23. Rosokha YS, Lindeman SV, Rosokha SV, Kochi JK (2004) Angew Chem Int Ed 43:4650
24. Han B, Lu JJ, Kochi JK (2008) Cryst Growth Des 8:1327
25. Hoog P, Gamez P, Mutikainen H, Turpeinen U, Reedijk J (2004) Angew Chem Int Ed 43:5815
26. Estarellas C, Rotger MC, Capó M, Quiñonero D, Frontera A, Costa A, Deyà PM (2009) Org Lett 11:1987
27. Mascal M, Yakovlev I, Nikitin EB, Fettinger JC (2007) Angew Chem Int Ed 46:8782
28. Chifotides HT, Schottel BL, Dunbar KR (2010) Angew Chem Int Ed 49:7202
29. Campos-Fernandez CS, Schottel BL, Chifotides HT, Bera JK, Bacsa J, Koomen JM, Russell DH, Dunbar KR (2005) J Am Chem Soc 127:12909
30. Berryman OB, Hof F, Hynes MJ, Johnson DW (2006) Chem Commun 506
31. Berryman OB, Sather AC, Hay BP, Meisner JS, Johnson DW (2008) J Am Chem Soc 130:10895
32. Gil-Ramirez G, Escudero-Adan EC, Benet-Buchholz J, Ballester P (2008) Angew Chem Int Ed 47:4114
33. Mareda J, Matile S (2009) Chem Eur J 15:28
34. Gorteau V, Bollot G, Mareda J, Matile S (2007) Org Biomol Chem 5:3000
35. Gorteau V, Bollot G, Mareda J, Perez-Velasco A, Matile S (2006) J Am Chem Soc 128:14788
36. Gorteau V, Julliard MD, Matile S (2008) J Membr Sci 321:37
37. Perez-Velasco A, Gorteau V, Matile S (2008) Angew Chem Int Ed 47:921
38. Dawson RE, Hennig A, Weimann DP, Emery D, Ravikumar V, Montenegro J, Takeuchi T, Gabutti S, Mayor M, Mareda J, Schalley CA, Matile S (2010) Nature Chem 2:533
39. Jentzsch AV, Emery D, Mareda J, Metrangolo P, Resnati G, Matile S (2011) Angew Chem Int Ed 50:11675
40. Sakai N, Mareda J, Vauthey E, Matile S (2010) Chem Commun 46:4225
41. Estarellas C, Frontera A, Quiñonero D, Deyà PM (2011) Angew Chem Int Ed 50:415
42. Estarellas C, Frontera A, Quiñonero D, Deyà PM (2011) Chem Asian J 6:2316
43. Schottel BL, Chifotides HT, Dunbar KR (2008) Chem Soc Rev 37:68
44. Caltagirone C, Gale PA (2009) Chem Soc Rev 38:520
45. Robertazzi A, Krull F, Knapp E-W, Gamez P (2011) CrystEngComm 13:3293
46. Garau C, Frontera A, Quiñonero D, Ballester P, Costa A, Deyà PM (2003) ChemPhysChem 4:1344
47. Alkorta I, Blanco F, Deyà PM, Elguero J, Estarellas C, Frontera A, Quiñonero D (2010) Theor Chem Acc 126:1
48. Estarellas C, Frontera A, Quiñonero D, Deyà PM (2011) ChemPhysChem 12:2742
49. Gural'skiy IA, Escudero D, Frontera A, Solntsev PV, Rusanov EB, Chernega AN, Krautscheid H, Domasevitch KV (2009) Dalton Trans 2856
50. Kollman PA (1972) J Am Chem Soc 94:1837
51. Sannigrahi AB, Kar T, Niyogi BG, Hobza P, Schleyer PvR (1990) Chem Rev 90:1061
52. Li Q, Hu T, An X, Li W, Cheng J, Gong B, Sun J (2009) ChemPhysChem 10:3310
53. Bader RFW (1998) J Phys Chem A 102:7314
54. Ahlrichs R, Bär M, Hacer M, Horn H, Kömel C (1989) Chem Phys Lett 162:165
55. Peterson KA, Puzzarini C (2005) Theor Chem Acc 114:283
56. Figgen D, Rauhut G, Dolg M, Stoll H (2005) Chem Phys 311:227
57. Feyereisen MW, Fitzgerald G, Komornicki A (1993) Chem Phys Lett 208:359
58. Vahtras O, Almlof J, Feyereisen MW (1993) Chem Phys Lett 213:514
59. Frontera A, Quiñonero D, Garau C, Ballester P, Costa A, Deyà PM (2005) J Phys Chem A 109:4632
60. Quiñonero D, Garau C, Frontera A, Ballester P, Costa A, Deyà PM (2006) J Phys Chem A 110:5144
61. Quiñonero D, Estarellas C, Frontera A, Deyà PM (2011) Chem Phys Lett 508:144
62. Geronimo I, Singh NJ, Kim KS (2011) J Chem Theory Comput 7:825
63. Boys SF, Bernardi F (1970) Mol Phys 19:553
64. Bader RFW (1991) Chem Rev 91:893
65. Biegler-König F, Schönbohm J, Bayles D (2001) J Comp Chem 22:545
66. Sigfridson E, Ryde U (1998) J Comput Chem 19:377
67. Ding L, Wagner M, Bolte M (2001) Acta Crystallogr Sect C: Cryst Struct Commun 57:162
68. Ma K, Bats JW, Wagner M (2001) Acta Crystallogr Sect E: Struct Rep Online 57:o846
69. Buttery JHN, Effendy Mutrofin S, Plackett NC, Skelton BW, Whitaker CR, White AHZ (2006) Anorg Allg Chem 632:1851
70. Wheeler SE, Houk KN (2010) J Phys Chem A 114:8658
71. Frontera A, Gamez P, Mascal M, Mooibroek T, Reedijk J (2011) Angew Chem Int Ed 50:9564
72. Wheeler SE, Houk KN (2009) J Am Chem Soc 131:3126
73. Wheeler SE (2011) J Am Chem Soc 133:10262
74. Estarellas C, Frontera A, Quiñonero D, Deyà PM (2011) J Phys Chem A 115:7849
75. Jonas V, Frenking G, Reetz MT (1994) J Am Chem Soc 116:8741
76. Lias SG, Bartmess JE, Liebman JF, Holmes JL, Levin R, Mallard WG (1988) J Phys Chem Ref Data 17(Suppl):1
77. Quiñonero D, Garau C, Frontera A, Ballester P, Costa A, Deyà PM (2002) Chem Phys Lett 359:486
78. Lucas X, Estarellas C, Escudero D, Frontera A, Quiñonero D, Deyà PM (2009) ChemPhysChem 10:2256
79. Escudero D, Frontera A, Quiñonero D, Deyà PM (2009) J Comput Chem 30:75
80. Vijay D, Zipse H, Sastry GN (2008) J Phys Chem B 112:8863